Nuclear Stopping from 0.09A to 1.93A GeV and Its Correlation to Flow

W. Reisdorf,[1] A. Andronic,[1] A. Gobbi,[1] O. N. Hartmann,[1] N. Herrmann,[2] K. D. Hildenbrand,[1] Y. J. Kim,[1,3] M. Kirejczyk,[1,4] P. Koczoń,[1] T. Kress,[1] Y. Leifels,[1] A. Schüttauf,[1] Z. Tymiński,[1,4] Z. G. Xiao,[1] J. P. Alard,[5] V. Barret,[5] Z. Basrak,[6] N. Bastid,[5] M. L. Benabderrahmane,[2] R. Čaplar,[6] P. Crochet,[5] P. Dupieux,[5] M. Dželalija,[6] Z. Fodor,[7] Y. Grishkin,[8] B. Hong,[3] J. Kecskemeti,[7] M. Korolija,[6] R. Kotte,[9] A. Lebedev,[8] X. Lopez,[5] M. Merschmeyer,[2] J. Mösner,[9] W. Neubert,[9] D. Pelte,[2] M. Petrovici,[10] F. Rami,[11] B. de Schauenburg,[11] Z. Seres,[7] B. Sikora,[4] K. S. Sim,[3] V. Simion,[10] K. Siwek-Wilczyńska,[4] V. Smolyankin,[8] M. Stockmeier,[2] G. Stoicea,[10] P. Wagner,[11] K. Wiśniewski,[4] D. Wohlfarth,[9] I. Yushmanov,[12] and A. Zhilin[8]

(FOPI Collaboration)

[1]*Gesellschaft für Schwerionenforschung, Darmstadt, Germany*
[2]*Physikalisches Institut der Universität Heidelberg, Heidelberg, Germany*
[3]*Korea University, Seoul, South Korea*
[4]*Institute of Experimental Physics, Warsaw University, Warsaw, Poland*
[5]*Laboratoire de Physique Corpusculaire, IN2P3/CNRS, and Université Blaise Pascal, Clermont-Ferrand, France*
[6]*Rudjer Boskovic Institute, Zagreb, Croatia*
[7]*Central Research Institute for Physics, Budapest, Hungary*
[8]*Institute for Theoretical and Experimental Physics, Moscow, Russia*
[9]*Forschungszentrum Rossendorf, Dresden, Germany*
[10]*National Institute for Nuclear Physics and Engineering, Bucharest, Romania*
[11]*Institut de Recherches Subatomiques, IN2P3-CNRS, Université Louis Pasteur, Strasbourg, France*
[12]*Kurchatov Institute, Moscow, Russia*

(Received 13 October 2003; published 11 June 2004)

We present a complete systematics (excitation functions and system-size dependences) of global stopping and side flow for heavy ion reactions in the energy range between 0.09A and 1.93A GeV. For the heaviest system, Au + Au, we observe a plateau of maximal stopping extending from about 0.2A to 0.8A GeV with a fast drop on both sides. The degree of stopping, which is shown to remain significantly below the expectations of a full stopping scenario, is found to be highly correlated to the amount of side flow.

DOI: 10.1103/PhysRevLett.92.232301 PACS numbers: 25.75.Ld, 25.70.Pq

In the last two decades collisions between accelerated heavy ions have become a major laboratory tool in large scale efforts to learn more about the properties of hot and compressed nuclear matter. Nuclei are small objects, however: from the Bethe-Weizsäcker formula describing empirical nuclear masses it follows that surface and Coulomb effects, which are not present in the interior of macroscopic nuclear objects, such as neutron stars, reduce the bulk binding energy per nucleon of 16 MeV to about half the value, i.e., 8 MeV. For this reason the one-fluid hydrodynamics approaches [1–3] that were favored in the early days to link experimental observations and fundamental properties of nuclear matter, such as the relation among pressure, density, and temperature [equation of state (EOS)] were not trivially justified. The first convincing evidence of collective (side) flow [4,5] raised hopes that this connection could be established successfully [6]. Meanwhile, flow phenomena in heavy ion reactions have been studied extensively [7]. With the advent in the mid 1980s of event simulation codes implementing microscopic transport theory [8] it soon became clear that nonequilibrium effects in such reactions could not be ignored. In one of the most recent attempts [9] to derive constraints on the EOS from heavy ion data(which also mentions some of the earlier works) it is made clear that progress on this topic requires improved understanding of the momentum dependence of the mean fields generated in a heavy ion collision (first introduced in Refs. [10,11]) as well as an extensive adjustment to experimental information on the degree of stopping achieved.

This Letter presents a complete systematics of stopping properties in heavy ion collisions at SIS energies. Our data show that the degree of stopping achieved in a heavy ion collision (i) reaches a well-defined plateau of maximal stopping centered around $0.5A \pm 0.3A$ GeV with a fast drop on both edges, (ii) stays significantly below the hydrodynamic limit at all energies, and (iii) shows a strong correlation to the global side flow suggesting that parametric adjustments to both observables might require an iterative procedure.

The experiments were performed at the heavy ion accelerator SIS of GSI/Darmstadt using the large acceptance FOPI detector [12]. A total of 25 system energies are analyzed for this work (energies in A GeV are given

in parentheses): ^{40}Ca + ^{40}Ca (0.4, 0.6, 0.8, 1.0, 1.5, 1.93), ^{58}Ni + ^{58}Ni (0.09, 0.15, 0.25, 0.4), ^{96}Ru + ^{96}Ru (0.4, 1.5), ^{129}Xe + ^{133}Cs^{127}I (0.15, 0.25, 0.4), ^{197}Au + ^{197}Au (0.09, 0.12, 0.15, 0.25, 0.4, 0.6, 0.8, 1.0, 1.2, 1.5). Particle tracking and energy loss determinations are done using two drift chambers, the CDC (covering polar angles between 35° and 135°) and the Helitron (9° − 26°), both located inside a superconducting solenoid operated at a magnetic field of 0.6 T. A set of scintillator arrays, Plastic Wall (7°–30°), Zero Degree Detector (1.4°–7°), and Barrel (42°–120°), allow us to measure the time of flight and, below 30°, also the energy loss. For the low-energy experiments (up to 0.4A GeV) the Helitron was replaced by an array of gas ionization chambers [13] allowing charge identification of heavier clusters. The velocity resolution below 30° was (0.5–1.5)%; the momentum resolution in the CDC was (4–12)% for momenta of 0.5 to 2 GeV/c, respectively. Use of CDC and Helitron allows the identification of pions, as well as good isotope separation for hydrogen and helium clusters in a large part of momentum space. Heavier clusters are separated by nuclear charge.

Collision centrality selection was obtained by binning distributions of either the detected charge particle multiplicity, MUL, or the ratio of total transverse to longitudinal kinetic energies in the center-of-mass (c.m.) system, *Erat*.

The scaled directed flow is $p_{x\mathrm{dir}}^{(0)} \equiv p_{x\mathrm{dir}}/u_{1\,\mathrm{c.m.}}$, where $p_{x\mathrm{dir}} = \sum \mathrm{sgn}(y) Z u_x / \sum Z$ (Z is fragment charge, $u_{1\,\mathrm{c.m.}}$ is the spatial part of the c.m. projectile 4-velocity, and $u_x \equiv \beta_x \gamma$ is the projection of the fragment 4-velocity on the reaction plane [14]). The sum is over all measured charged particles with $Z < 10$, excluding pions, and y is the c.m. rapidity. In the left panels of Fig. 1 we show the scaled impact parameter, $b^{(0)} = b/b_{\mathrm{max}}$, dependence of $p_{x\mathrm{dir}}^{(0)}$ for three system energies, ^{40}Ca + ^{40}Ca at 0.4A GeV, and ^{197}Au + ^{197}Au (0.4A and 1.5A GeV). We take $b_{\mathrm{max}} = 1.15(A_P^{1/3} + A_T^{1/3})$ fm and estimate b from the measured differential cross sections for the *Erat* or the multiplicity distributions, using a geometrical sharp-cut approximation. The *Erat* selections show better impact parameter resolution for the most central collisions than the multiplicity selections. The maximum value of $p_{x\mathrm{dir}}^{(0)}$ is a robust observable that does not depend significantly on both the selection method and the apparatus filter. For a comparative study of alternate, more differential measures of side flow in the published literature we refer to the reviews [7].

To obtain information on the degree of stopping, we measure rapidity distributions of the emitted particles. In an XYZ Cartesian coordinate system with the Z axis oriented in the beam direction and the X axis in the reaction plane, we define the (conventional) longitudinal rapidity distribution in the beam direction, and the transverse rapidity averaged over the X and Y directions by projecting on a transverse laboratory fixed axis. All rapidities are in the c.m. and are scaled by the beam rapidity.

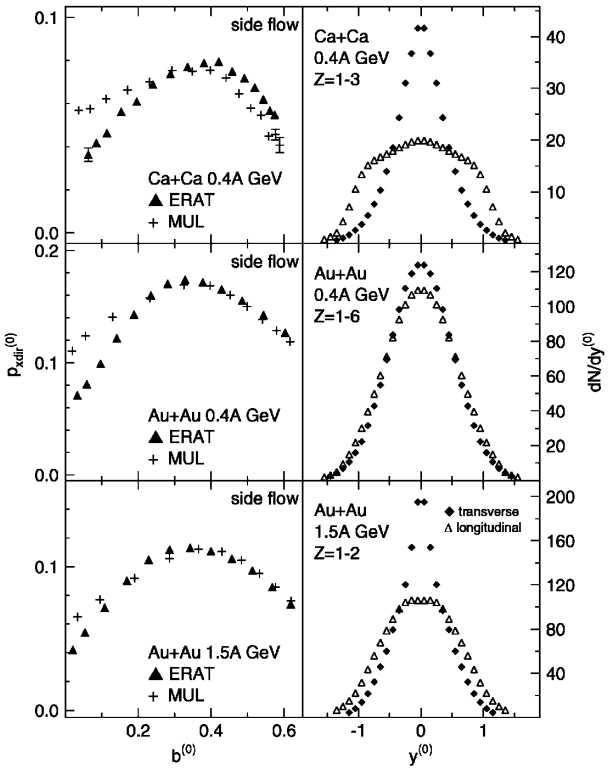

FIG. 1. Left panels: global side flow as a function of the scaled impact parameter (triangles: *Erat* selection; crosses: multiplicity selection). Right panels: global scaled transverse and longitudinal rapidity distributions for the *Erat* selection $b^{(0)} < 0.15$. Data for three indicated system energies are shown. Systematic errors are discussed in the text.

Results for the same system energies as in the left panels are shown in the right panels of Fig. 1.

The distributions are *full event* observables: all emitted charged baryonic particles are added, weighted with their respective nuclear charges. The total charge accounted for represents typically 95% of the system charge or more, except for data below 150A MeV, where threshold effects prevent complete coverage of fragments with charge $Z > 6$. Where necessary, bidimensional fitting procedures in u_t vs y space, which require reflection symmetry, have been used [15] to interpolate and partially extrapolate the measured spectra ($u_t \equiv \beta_t \gamma$ transverse 4-velocity; $y \equiv y_z$ longitudinal rapidity). Extrapolation corrections to obtain 4π distributions were less than 10% for protons and clusters with nuclear charge $Z = 1, 2$ and up to a maximum of 30% for heavier fragments.

As a measure of the degree of stopping we present data for an observable dubbed *vartl*, the ratio of the variances of the transverse to that of the longitudinal rapidity distributions. For an isotropic thermal source *vartl* should be equal to unity. Flow and transparency may change *vartl* however. Early, ideal hydrodynamics estimates [1] predict in this energy regime the phenomenon of *squeeze out,* resulting, for *central* collisions, in enhanced emission at polar (c.m.) angles of 90°: *vartl*

then becomes significantly larger than unity. To avoid the uncertainties and distortions of the measured far-out tails of these distributions, we limit the integration to the interval between $+1$ and -1 in the scaled values. By definition *Erat* and *vartl* are related, although technically different. Autocorrelations in *vartl*, as well as $p_{x\mathrm{dir}}$, were avoided by removing the particle of interest from the selection criterion *Erat* or, respectively, the transverse-momentum vector [14] determining the reaction plane.

The observable *vartl* is also related in spirit to $R = (2/\pi)\sum|p_{ti}|/\sum|p_{zi}|$ suggested in Ref. [16] and used in earlier stopping studies [17]. Longitudinal rapidity distributions for selected particles, measured with the PLASTIC BALL [17] were published [18] for a limited set of systems and beam energies.

At this point we note that all statistical errors in this work are significantly smaller than the systematic errors. Estimates of the latter, varying between 5% and 12% for the rapidity distributions, are based on comparisons of measured yields in the c.m. backward/forward hemispheres, checks of the overall charge balance, and technical variations of the fitting procedure. For $p^{(0)}_{x\mathrm{dir}}$ (*vartl*) a constant uncertainty of 0.008 (0.04) describes best the overall error. Point-by-point fluctuations (shown in Fig. 2) are smaller: 0.005 (0.02). Simulations with the transport code IQMD (based on quantum molecular dynamics [19]), together with detector filters, were also used to assess these errors.

The upper-left panel of Fig. 2 shows excitation functions of *vartl* for Au + Au and Ca + Ca in central collisions corresponding to scaled impact parameters $b^{(0)} < 0.15$. Interesting aspects of these data are (a) the occurrence, for Au + Au, of a plateau of maximal stopping extending from $0.2A$ to $0.8A$ GeV with a fast drop on both sides, (b) the fact that *vartl* never reaches values above or even close to unity, and (c) the large system-size dependence evidenced by comparing the Au + Au with the Ca + Ca data.

The smaller values for the lighter system offer a key argument in favor of interpreting $vartl < 1$ as evidence for partial transparency, rather than the dominance of longitudinal over transversal pressure gradients.

More detailed information on the system-size dependence at two incident beam energies ($0.4A$ and $1.5A$ GeV) is shown in the upper right panel of Fig. 2 which also demonstrates that, especially at the lower energy, there is no evident saturation as one goes from Ca + Ca, via Ni + Ni, Ru + Ru, and Xe + CsI, all the way to Au + Au.

The two lower panels of the Fig. 2 show by comparison with the two upper panels an impressive correlation with the maximum (see Fig. 1) scaled directed side flow, $\max[p^{(0)}_{x\mathrm{dir}}]$, both in the excitation functions and in the size dependence. In particular, side flow is *positively* correlated with *vartl* as shown in Fig. 3 for 22 system energies (data for $E/A < 0.15$ GeV were omitted because only upper limits on *vartl* could be determined).

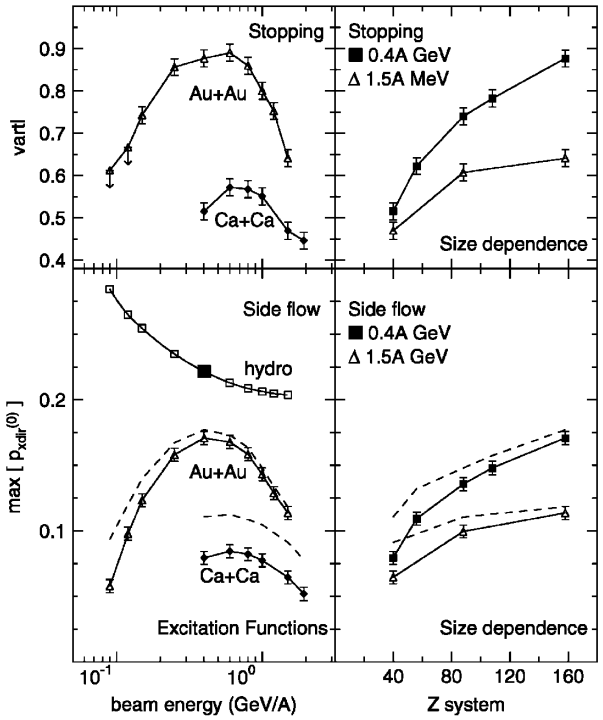

FIG. 2. Excitation functions (left) and size dependences (right) of the degree of stopping (upper panels) and maximal global side flow (lower panels). The dashed curves result from a correction for statistical fluctuations in the reaction plane orientation. The curve labeled "hydro" is an estimate of the hydrodynamic limit for the side flow. See the text.

Although the two global observables are measured at different average impact parameters, the most natural explanation of the observed correlation is that side flow is resulting from the pressure gradient between participant and spectator matter, which in turn grows with the degree of stopping. Note that properly scaled side flow is essential to reveal this correlation. Both observables are also expected to be influenced by the statistics of elementary collisions. The estimated [20] effect on side flow is shown in Fig. 2.

Using the Rankine-Hugoniot-Taub one-dimensional shock equations together with a realistic equation of state (SLy230a from Ref. [21]), we have estimated the maximal densities and pressures $\mathcal{P}$ to be expected under the full stopping assumption for the energy regime of interest here. Characterizing the system size by R_{sys} and the (passing) time by t_{pass}, the scaled global side flow should behave as $\mathrm{grad}\mathcal{P} \times t_{\mathrm{pass}}/u_{1\,\mathrm{c.m.}} \approx (\mathcal{P}/R_{\mathrm{sys}})(R_{\mathrm{sys}}/u_{1\,\mathrm{c.m.}})/u_{1\,\mathrm{c.m.}} = \mathcal{P}/u^2_{1\,\mathrm{c.m.}}$. The latter quantity, with a normalization to be discussed below, is plotted in Fig. 2 (lower left panel) and compared to the measured scaled side flow. Note that ideal-gas one-fluid hydrodynamics predicts [22] a size independent flat excitation function (R_{sys} drops out, and $\mathcal{P}$ rises linearly with $u^2_{1\,\mathrm{c.m.}}$).

Our estimate of the shape of the excitation function does not yield the absolute value of $\max[p^{(0)}_{x\mathrm{dir}}]$, which

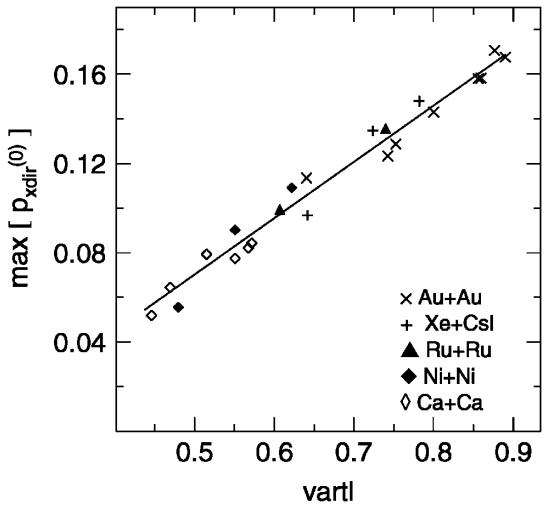

FIG. 3. Correlation between the maximal directed side flow and the degree of stopping. The line is a linear least squares fit to the data, which extend from 0.15*A* to 1.93*A* GeV.

depends on the geometrical details of the collision. We opted for an estimate of the normalization by performing an IQMD calculation using, instead of the free-space nucleon-nucleon elastic cross sections, values enhanced by a factor of 2 over the known free-space values, thus mocking up approximately the full stopping situation (we found $vartl = 1.23$, confirming qualitatively early predictions [1]). The resulting maximal side flow value (0.225 at 0.4*A* GeV) is marked by a full square in Fig. 3. This serves to give an idea of what to expect in the ideal hydrodynamics (nonviscous, one-fluid) limit. Introducing still higher elementary cross sections in the simulation does not change the prediction of *vartl* significantly as expected in the hydrodynamic limit and confirming the relevance of *vartl* to assess stopping.

The difference between the theoretical estimate and the experimental observation is likely to be the finite viscosity of hot nuclear matter, or, equivalently, the finite ratio $R_{\rm sys}/\lambda_f$ (which is the Reynolds number with λ_f the mean free path), which is not sufficiently large to produce fully macroscopic ideal hydrodynamic behavior in such collisions. The significant difference of typically 30% in the plateau region, together with the observed strong system-size dependence (already known from earlier studies [7,17] of the flow of selected ejectiles), stress the "small-object" character of nuclei: finite-size (surface) effects are large. The most interesting, and new, aspect of the full-event data, however, is the rapid drop away from the plateau. In particular, the gradual rise of the theoretical prediction at the low-energy end is totally suppressed by both the onset of partially attractive mean fields and the increase of Pauli blocking below 0.4*A* GeV [23]. On the high energy end (1.5*A* GeV) of our data, looking again at Fig. 2, one can estimate that the effective average pressures achieved are as much as a factor of 2 lower than the full-stop scenario would predict. In-medium modifications of elementary cross sections [24], caused possibly by nucleon-mass changes at high density, might be needed to account for the apparent rise of transparency in an energy regime where strong effects of Pauli blocking are no longer expected.

Our observation of partial transparency confirms qualitatively earlier isospin tracer experiments [25] and, together with its close correlation to side flow, has important consequences for the ongoing efforts to extract the equation of state from heavy ion data in the nonequilibrium situation [26], as well as for attempts to understand in-medium effects on mesonic and baryonic particles, since the effective densities in the early phase of the reactions are expected to be strongly correlated to the degree of stopping.

This work was partly supported by the German BMBF under Contracts No. 06HD953 and No. RUM-99/010 and by KRF under Grant No. 2002-015-CS0009.

[1] W. Scheid *et al.*, Phys. Rev. Lett. **32**, 741 (1974); W. Schmidt *et al.*, Phys. Rev. C **47**, 2782 (1993).
[2] H. Stöcker and W. Greiner, Phys. Rep. **137**, 277 (1986).
[3] R. B. Clare and D. Strottman, Phys. Rep. **141**, 177 (1986).
[4] H. A. Gustafsson *et al.*, Phys. Rev. Lett. **52**, 1590 (1984).
[5] R. E. Renfordt *et al.*, Phys. Rev. Lett. **53**, 763 (1984).
[6] G. Buchwald *et al.*, Phys. Rev. Lett. **52**, 1594 (1984).
[7] W. Reisdorf and H. G. Ritter, Annu. Rev. Nucl. Part. Sci. **47**, 663 (1997); N. Herrmann, J. P. Wessels, and T. Wienold, *ibid.* **49**, 581 (1999).
[8] G. F. Bertsch and S. Das Gupta, Phys. Rep. **160**, 189 (1988).
[9] P. Danielewicz, R. Lacey, and W. G. Lynch, Science **298**, 1592 (2002).
[10] J. Aichelin *et al.*, Phys. Rev. Lett. **58**, 1926 (1987).
[11] C. Gale *et al.*, Phys. Rev. C **35**, 1666 (1987).
[12] J. Ritman, Nucl. Phys. (Proc. Suppl.) **44**, 708 (1995).
[13] A. Gobbi *et al.*, Nucl. Instrum. Methods Phys. Res., Sect. A **324**, 156 (1993).
[14] P. Danielewicz and G. Odyniec, Phys. Lett. B **157**, 146 (1985).
[15] W. Reisdorf *et al.*, GSI Report No. 2001-1, p. 34 (http://www.gsi.de/annrep2001).
[16] H. Ströbele *et al.*, Phys. Rev. C **27**, 1349 (1983).
[17] H. H. Gutbrod, A. M. Poskanzer, and H. G. Ritter, Rep. Prog. Phys. **52**, 1267 (1989).
[18] H. H. Gutbrod *et al.*, Z. Phys. A **337**, 57 (1990).
[19] J. Aichelin, Phys. Rep. **202**, 233 (1991); C. Hartnack *et al.*, Eur. Phys. J. A **1**, 151 (1998).
[20] J.-Y. Ollitrault, Nucl. Phys. **A638**, 195 (1998).
[21] E. Chabanat *et al.*, Nucl. Phys. **A627**, 710 (1997).
[22] N. L. Balazs *et al.* Nucl. Phys. **A424**, 605 (1984).
[23] P. Danielewicz, Phys. Lett. B **146**, 168 (1984).
[24] G. Q. Li and R. Machleidt, Phys. Rev. C **48**, 1702 (1993); **49**, 566 (1994).
[25] F. Rami *et al.*, Phys. Rev. Lett. **84**, 1120 (2000); B. Hong *et al.*, Phys. Rev. C **66**, 034901 (2002).
[26] T. Gaitanos *et al.*, Nucl. Phys. **A650**, 97 (1999); C. Fuchs and T. Gaitanos, Nucl. Phys. **A714**, 643 (2003).